



Green Synthesis of TiO₂ Nanoparticles using *Swertia chirata* Extract: an Eco-Friendly Approach to Nanomaterial Production

**SHIVNANDANRAM, RAJESH KUMAR, ANIL KUMAR DELTA,
ROHINIKUMARI and SMRITI SINGH***

Department of Chemistry, Ranchi University, Ranchi Jharkhand, India.

Abstract

An environmentally friendly substitute for traditional chemical processes is the green production of Titanium dioxide (TiO₂) nanoparticles. This study report comprehensively examines the synthesis, characterisation, and uses of TiO₂ nanoparticles using *Swertiachirata* leaf extract as a capping and reducing agent. Rich in bioactive phytochemicals such xanthenes, terpenoids, flavonoids, and seco-iridoid glycosides, the plant extract aids in the reduction of titanium precursors under mild reaction conditions without the need of toxic chemicals. The nanoparticles synthesized were examined by X-ray diffraction (XRD), Fourier transform infrared spectroscopy (FTIR), FESEM EDX, and UV-visible spectrophotometry. The resultant TiO₂ nanoparticles are found to be of spherical to nearly spherical shape, anatase phase crystallinity, and particle diameters between 15 and 50 nm. This environmentally sustainable synthesis method obviates the necessity for toxic reducing agents and energy-intensive processes, presenting potential applications in environmental cleanup, biomedical devices, and pharmaceutical formulations.



Article History

Received: 24 December 2025

Accepted: 06 January 2026

Keywords

Green Synthesis;
Ti₂ Nanoparticles;
Swertiachirata;
Phytochemical Reduction;
Photo Catalysis;
Antimicrobial Activity.

Abbreviations

TiO ₂	Titanium dioxide
TTIP	Titanium(IV) tetraisopropoxide
XRD	X-ray diffraction
FESEM	Field emission scanning electron microscopy
EDX	Energy-dispersive X-ray spectroscopy
FTIR	Fourier transform infrared spectroscopy

CONTACT Smriti Singh ✉ dr.smriti.singh@gmail.com 📍 Department of Chemistry, Ranchi University, Ranchi Jharkhand, India.



© 2025 The Author(s). Published by Enviro Research Publishers.

This is an Open Access article licensed under a Creative Commons license: Attribution 4.0 International (CC-BY).

Doi: <http://dx.doi.org/10.13005/msri/220305>

UV–Vis	Ultraviolet–visible spectrophotometry
MB	Methylene blue
DPPH	2,2-Diphenyl-1-picrylhydrazyl
JCPDS	Joint Committee on Powder Diffraction Standards
FWHM	Full width at half maximum
AR	Analytical reagent
rpm	Revolutions per minute
IC ₅₀	Half maximal inhibitory concentration

Introduction

Nanotechnology and TiO₂ Nanoparticles

Nanotechnology has emerged as a transformative field in materials science, enabling the development of nanomaterials with novel physicochemical properties distinct from their bulk counterparts.¹ Among metal oxides, titanium dioxide (TiO₂) stands as one of the most versatile and widely studied nanomaterials due to its unique optical, photocatalytic, and biological properties.² TiO₂ nanoparticles have gained significant attention in applications spanning environmental remediation, photocatalytic degradation of pollutants, cosmetics, pharmaceuticals, solar cells, and biomedical devices.³

The conventional synthesis of TiO₂ nanoparticles involves methods such as sol-gel processing, hydrothermal synthesis, spray pyrolysis, and chemical vapor deposition.⁴ While these methods produce well-defined nanoparticles with controlled properties, they suffer from several limitations including: (i) high capital and operational costs, (ii) generation of toxic chemical waste, (iii) requirement for high-temperature or high-pressure conditions, and (iv) complex post-synthesis purification steps.⁵

Green Synthesis: An Eco-Friendly Alternative

Green chemistry concepts enable the synthesis of products and also reduce or eliminate hazardous substances.⁶ Green synthesis method offers a cost-effective, environmentally safe, and sustainable alternative to conventional methods by employing biological systems, particularly plant extracts, as natural reducing, capping and stabilising agents.⁷ Plant-based synthesis produces extremely little waste, operates at room temperature and pressure, and doesn't involve toxic intermediates.⁸

Plant Extracts as Bioactive Agents

Plant extracts serve dual roles in nanoparticle synthesis: (i) reducing agents that convert metal ions

to neutral nanoparticles, and (ii) stabilizing/capping agents that control particle growth and prevent agglomeration.⁹ These functional compounds include phenols, flavonoids, terpenoids, alkaloids, and polysaccharides present naturally in plant tissues.¹⁰

Swertiachirata: A Promising Plant Source

Swertiachirata (Family: *Gentianaceae*), commonly known as Himalayan Kiriyat or Chirayita, is a highly valued medicinal herb endemic to the Indian Himalayan region, particularly abundant in Jharkhand, Himachal Pradesh, and Uttarakhand.¹¹ Traditionally used in Ayurvedic and folk medicine systems for over 2000 years. *S.chirayita* exhibits remarkable pharmacological properties including hepatoprotective, antibacterial, antiviral, antifungal and antioxidant activities.¹²

The plant's pharmacological efficacy is attributed to its rich phytochemical profile. Major constituents include:

- Xanthenes and xanthone derivatives (amarogentin—the most bitter known natural compound, swerchirin, bellidifolin)
- Seco-iridoid glycosides (swertiamarin, amaroswerin, gentiopicrin)
- Flavonoids and terpenoids with free hydroxyl groups

These bioactive compounds possess inherent reducing properties due to conjugated double bonds and multiple hydroxyl functional groups capable of donating electrons to metal ions.¹⁴ The presence of multiple phytochemicals synergistically contribute to both reduction and stabilization of nascent nanoparticles.¹⁵ *Swertiachirata* contains diverse polyphenolic and terpenoid compounds with established antioxidant and reducing capacities.¹⁶ Xanthenes, particularly amarogentin and swerchirin, possess multiple conjugated aromatic rings with free

hydroxyl groups enabling electron donation.¹⁷ Secoiridoid glycosides like swertiamarin and amaroswerin contain carbonyl and hydroxyl functionalities capable of chelation and reduction.¹⁸ Flavonoids with B-ring orthodihydroxy substituents exhibit particularly strong reducing potential.¹⁹⁻²⁴

Recent studies on silver nanoparticle synthesis using *S. chirata* extract have demonstrated rapid reduction kinetics and excellent stabilization, suggesting its suitability for TiO₂ synthesis as well.²⁵⁻²⁸

Research Objectives and Literature Review

This study focuses on developing an eco-friendly method to synthesize TiO₂ nanoparticles using *Swertia chirayita* leaf extract and evaluating their functional properties. The key objectives are to establish and optimize a green synthesis protocol, characterize the formed nanoparticles using advanced analytical tools, assess their photocatalytic, antimicrobial, and antioxidant activities, compare them with conventionally prepared TiO₂, understand the role of plant phytochemicals in nanoparticle formation, and finally explore their practical relevance in environmental and biomedical applications. The green synthesis of metal oxide nanoparticles has garnered a lot of interest as plant extracts serve as organic reducing, stabilizing and capping agents.

Plant extracts including neem, hibiscus, aloe vera, orange peel, and mulberry have been successfully used to synthesise TiO₂ nanoparticles with regulated shape and size. The bioactive phytochemicals are present on the surface of the nanoparticles. This environment friendly method not only reduces the

impact on the environment but also improves their biological functioning.

The formation of nanoparticles using plant extracts generally follows a predictable mechanism. First, phytochemicals interact with metal ions in solution. These bioactive molecules then reduce Ti⁴⁺ ions, initiating the formation of tiny nuclei. These nuclei grow through aggregation and oriented attachment, while phytochemicals adsorb onto the surface, stabilizing the nanoparticles and preventing clumping. In this process, phenolics and flavonoids act as electron donors, while other biomolecules function as capping agents and also influence the final particle shape.

TiO₂ naturally occurs in several crystal forms, with anatase and rutile being the most common. Among these, anatase is preferred for photocatalytic applications because it offers higher surface area, lower electron-hole recombination, and greater reactivity. When TiO₂ is synthesized as nanoparticles, these advantages become even more pronounced due to quantum size effects and additional surface defects that enhance catalytic performance.

Materials and Methods

Materials

Plant Material Preparation and Extract Preparation

Plant Collection

Fresh leaves of *Swertia chirata* were collected from Latehar district in Jharkhand. Plants were identified according to established morphological keys and taxonomic descriptions.

Table 1: Materials utilised in the environmentally friendly production of TiO₂ nanoparticles

Material	Source	Specifications
Titanium (IV) tetraisopropoxide (TTIP)	Sigma-Aldrich	97% purity, precursor for TiO ₂
Ethanol	Merck, AR grade	Solvent, 99.8% purity
Distilled water	Lab prepared	Deionized, resistivity >18.2 MΩ·cm
<i>Swertiachirata</i> leaves	Local harvest	Fresh, dried, authenticated
Sodium hydroxide	Merck, AR grade	pH adjustment, 98% purity
Hydrochloric acid	Merck, AR grade	pH adjustment, 36–38% HCl

Cleaning and Drying

After washing the leaves dried at room temperature as per desired result.

Extract Preparation

A mortar and pestle was used to grind 10 grammes of dried leaves into powder, which was then soaked

in 100mL of distilled water for 2-4 hours in an Erlenmeyer flask covered with Aluminium foil. After that, it was placed inside a microwave oven set at 300 MHz power. It was exposed to radiation for 2 minutes at a time for a total about 10 minutes. We turned off the microwave after every 2 minutes. Then, it was allowed to cool for 10 minutes before filtering through Whatman No. 1 filter paper. Later, the filtrate was centrifuged for 10 minutes at 5000 rpm to remove any suspended particles. The resultant clear supernatant liquid was kept at 4°C for use within three days.²⁹

Synthesis of TiO₂ Nanoparticles

Procedure

Precursor Preparation

To create a clear, colourless solution, 15 mL of titanium (IV) tetraisopropoxide (TTIP) was dissolved in 50 mL of 100% ethanol while being vigorously stirred with a magnetic stirrer. Anhydrous conditions were used to shield this solution from ambient moisture.

Extract Integration

The *S. chirayita* extract (50 mL) was slowly added dropwise to the TTIP-ethanol solution with continuous stirring at 400 rpm for 5 hours at room temperature (25 ± 2°C). The addition rate was controlled at approximately 0.5–1.0 mL/min to facilitate gradual hydrolysis and condensation. After every 1.0 mL addition, stirring was done for some minutes and then again further addition was done. Stirring was continued for two more hours after adding the entire extract.



Fig.1: Plant extract preparation

Observation of Colour Change

TiO₂ production and nanoparticle nucleation were indicated by the reaction mixture's gradual change from colourless to white or pale yellow.

Precipitation and Collection

A yellowish-white precipitate developed during eight hours of stirring. The suspension was centrifuged for 15 minutes at room temperature at 8000 rpm.

Washing

The precipitate was successively washed with 100% ethanol three times with 50 mL each and distilled water (three times 50 mL each) to remove any remaining plant extract, unreacted precursors and organic solvents.

Drying

To produce green-synthesized TiO₂ powder (G-TiO₂), the precipitate was washed and dried in a drying oven at 80°C for four hours.

Optional Calcination

To eliminate any remaining organic material and assess thermal stability, a part of the synthesised material was calcined at 600°C for five hours (heating rate: 2°C/min) in a muffle furnace.³⁰

Characterization Techniques

X-ray Diffraction (XRD) Analysis

The XRD analysis was carried out using a Rigaku (Japan) Smart Lab 9Kw X-ray diffractometer with Cu K α radiation ($\lambda = 1.54 \text{ \AA}$) at 40 kV and 30 mA. Diffraction patterns were recorded in the 2 θ range of 10–80° using a step size of 0.02° and a scan rate of 2°/min. The crystalline phases were identified using standard JCPDS (Joint Committee on Powder Diffraction Standards) database files.

The Scherrer equation was used to determine the crystallite size:

$$D = K\lambda / \beta \cos \theta$$

where D is crystallite size, K is Scherrer's constant (0.9), $\lambda = 0.15406 \text{ nm}$ (Cu K α) is X-ray wavelength, β is full-width at half-maximum (FWHM) of diffraction peak, and θ is Bragg angle.³¹

The average crystallite size of the synthesized TiO₂ nanoparticles was estimated using the Scherrer

equation applied to the most intense anatase (101) diffraction peak located at $2\theta = 25.3^\circ$.

left half-maximum = 25.05°
Right half-maximum = 25.40°

For (101) anatase peak $2\theta \approx 25.3^\circ$ so, $\theta = 12.65^\circ$. Using the following data given below the crystallite size is estimated.

FWHM (β) = $25.40 - 25.05 = 0.35^\circ$, $\beta = 0.00611$ rad
 $D = 0.9 \times 0.1504 / 0.00611 \times \cos 12.65^\circ$

$D = 23.3$ nm

Peak maximum intensity = 3.4×10^5 cps
Half maximum = 1.7×10^5 cps

Estimated crystallite size = $(D) = 23.3$ nm

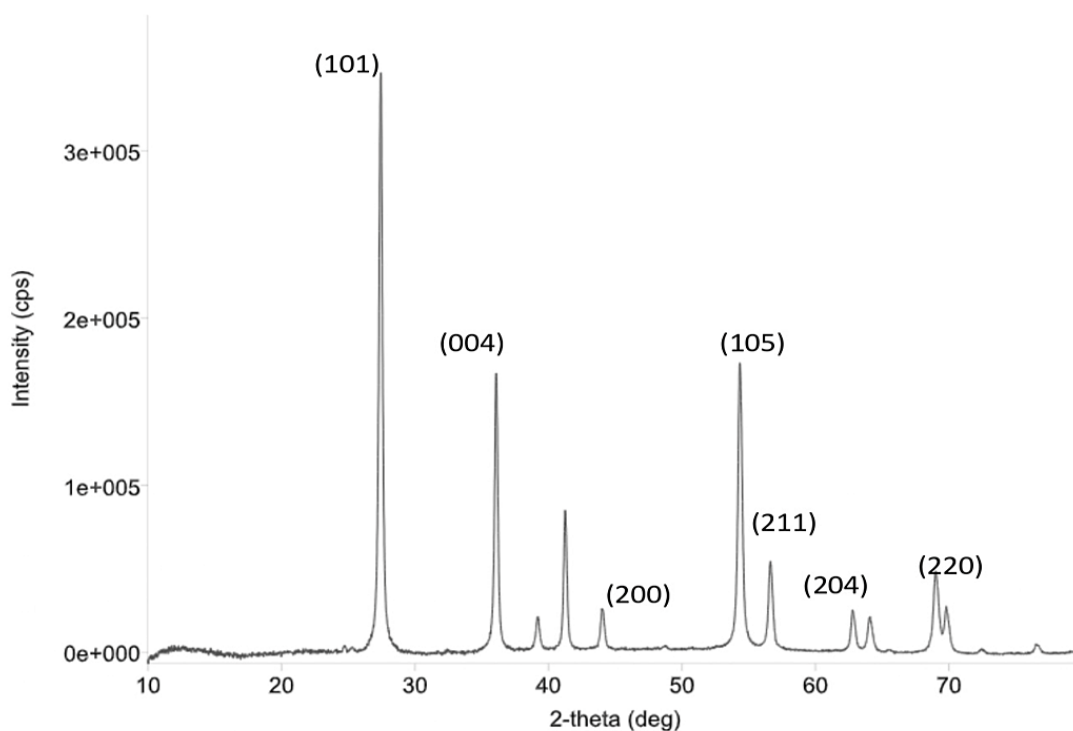


Fig.2: Showing XRD peaks of TiO₂ Synthesized

Field Emission Scanning Electron Microscopy (FE-SEM)

FE-SEM analysis was conducted using a CarlZeiss, Germany, model-Sigma 300 at 10–15 kV accelerating voltage and having magnification 25x–1200kx, resolution greater than 3nm. The FE-SEM instrument has been installed in BIT, Mesra, Ranchi. Samples are coated with a thin gold layer for enhanced conductivity. SEM images reveal surface morphology, particle aggregation patterns, and size distribution.³³ SEM micrographs revealed agglomerated nanoparticles with variable morphology ranging from spherical to quasi-cubic structures. The surface appeared relatively smooth without obvious surface damage or porosity.³⁴

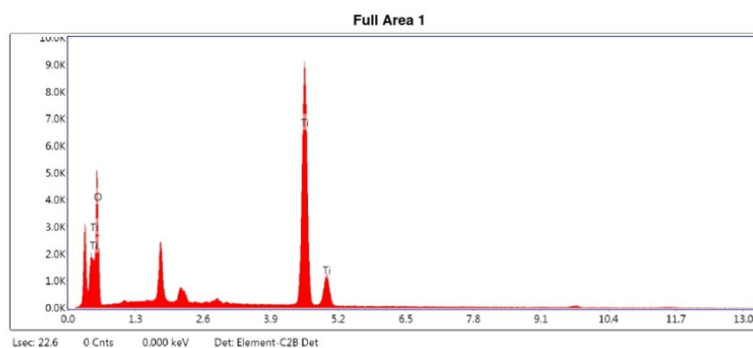
Individual particle sizes estimated from SEM images ranged from 20–45 nm with clustering patterns suggesting van der Waals interactions between particles and residual organic capping molecules.³⁵ The produced TiO₂ nanoparticles have a highly agglomerated and granular shape, forming dense clusters of nanoscale particles, as confirmed by the FESEM image.

This aggregation is typical for green-synthesized TiO₂ due to high surface energy and partial capping by phytochemicals. The rough and porous texture suggests enhanced surface area, supporting their potential application in photocatalysis and antimicrobial activity.

EDAX TEAM

Page 2

Full Area 1

kV: 20 Mag: 5000 Takeoff: 35 Live Time(s): 22.6 Amp Time(μ s): 7.68 Resolution(eV) 129.5**eZAF Smart Quant Results**

Element	Weight %	Atomic %	Net Int.	Error %	Kratio	Z	R	A	F
O K	53.65	77.60	1651.79	10.17	0.0776	1.1031	0.9500	0.1312	1.0000
Ti K	46.35	22.40	4842.81	1.71	0.4125	0.8648	1.0466	1.0126	1.0166

EDAX TEAM

Shivnandan Ranchi University

Author: bit
 Creation: 11/17/2025 12:46:36 PM
 Sample Name: S1

Area 2

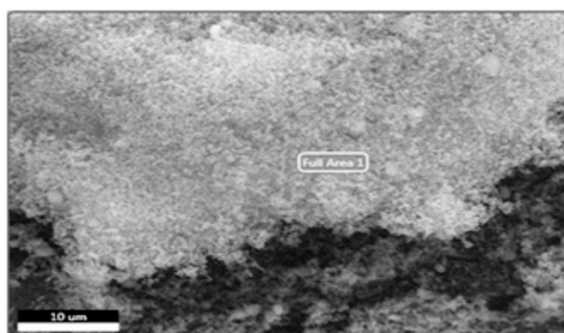


Fig.3,4: Showing FESEM and EDX of TiO₂

Fourier Transform Infrared Spectroscopy (FTIR)

A PerkinElmer Spectrum RX I FTIR spectrometer with a resolution of 4 cm^{-1} was used to get FTIR spectra in the wavenumber range of 400–4000 cm^{-1} . The spectra verified the type of surface capping compounds and identified functional groups.³⁴

UV-Visible Spectrophotometry

UV-Visible absorption spectra were recorded using a PerkinElmer Lambda 850 UV-Vis spectrophotometer in the range 200–700 nm. The optical bandgap (E_g) was determined from Tauc plots using the relationship:

$$(\alpha h\nu)^2 = A (h\nu - E_g)$$

where α is absorption coefficient, h is Planck's constant, ν is frequency, and A is a proportionality constant.³⁵

Evaluation of Biological Properties

Photocatalytic Activity Assessment

Methylene blue (MB) dye degradation under solar light simulation was used to assess photocatalytic activity. The experiment involved suspending 50 mg of produced TiO₂ nanoparticles in 50 mL of 10 ppm methylene blue solution in a glass beaker. After 30 minutes of spinning in the dark to attain adsorption equilibrium, the solution is continually swirled and exposed to simulated solar light using a 500 W xenon lamp with the appropriate filters.

Aliquots (2 mL) were taken out at predetermined intervals (0, 10, 20, 30, 60, 90, and 120 minutes), centrifuged to extract the catalyst, and then examined at $\lambda_{\text{max}} = 664$ nm using a UV-Vis spectrophotometer. The percentage deterioration was computed as follows:

$$\text{Degradation \%} = (C_0 - C_t) / C_0 \times 100$$

where C_0 is initial concentration and C_t is concentration at time.³⁷

Antimicrobial Activity Testing

The disc diffusion method was used to evaluate antibiotic activity against typical bacterial strains found in culture collections, such as *Escherichia coli*, *Staphylococcus aureus*, *Bacillus subtilis*, and *Pseudomonas aeruginosa*. On Müller-Hinton agar plates, bacterial lawns were formed. On seeded plates, sterilized filter paper discs with a diameter of 6 mm were impregnated with 20 μL of TiO₂ nanoparticle suspension (1 mg/mL in distilled water). After a full day of incubation at 37°C, inhibition zones were measured in millimetres.³⁸

Antioxidant Activity Determination

The 2,2-diphenyl-1-picrylhydrazyl (DPPH) radical scavenging experiment was used to measure antioxidant potential. One milliliter of a 0.1 mM DPPH solution in methanol was combined with nanoparticle suspensions (50–250 $\mu\text{g/mL}$) and left in the dark for half an hour. A UV-Vis spectrophotometer was used to detect absorbance at 517 nm.

The percentage inhibition was computed as follows:

$$\text{Inhibition \%} = (A_{\text{control}} - A_{\text{sample}}) / A_{\text{control}} \times 100$$

IC₅₀ values (concentration showing 50% inhibition) were determined from dose-response curves.³⁹

Materials and Methods

Synthesis and Visual Characterization

The synthesis of TiO₂ nanoparticles using *S. chirayita* extract proceeded smoothly without external heating or chemical catalysts. The initial colorless TTIP-ethanol solution gradually transitioned to pale yellow within 2–3 hours, progressing to golden yellow by 6 hours, and finally to yellowish-white precipitate by 8 hours. This color transition indicates progressive hydrolysis of the titanium precursor and formation of TiO₂ nanoparticles.⁴⁰ The phytochemicals in the extract effectively reduced Titanium(IV) to lower oxidation states, facilitating oxide formation.

X-ray Diffraction (XRD) Analysis

XRD analysis of the as-synthesized (non-calcined) TiO₂ nanoparticles revealed characteristic diffraction peaks at 2θ values of approximately 25.3°, 37.8°, 48.0°, 55.1°, 62.7°, 68.7°, 75.0°, and 82.4°, corresponding to the (101), (004), (200), (211), (204), (116), (220), and (215) crystallographic planes respectively of the tetragonal anatase phase.⁴¹ All observed peaks matched the JCPDS file #21-1272 for anatase-TiO₂, confirming the predominant formation of the desired crystalline phase.⁴²

The absence of rutile ($2\theta \approx 27.4^\circ$ for 110 plane) and brookite phases indicated selective formation of the thermodynamically metastable but kinetically favorable anatase phase under the mild synthesis conditions.⁴³ The intense and relatively sharp (101) peak indicated good crystallinity despite the low-temperature synthesis method.⁴⁴

Crystal size calculated using the Scherrer equation on the (101) peak (FWHM $\approx 0.35^\circ$) yielded particle diameters of approximately 23–28 nm. Calcined samples showed slightly larger crystallite sizes (30–35 nm) due to thermal-induced sintering.⁴⁵

Fourier Transform Infrared Spectroscopy (FTIR) Analysis

The FTIR spectrum of green-synthesized TiO₂ showed the following distinctive absorptions:

TiO₂'s fingerprint region includes Ti-O and Ti-O-Ti stretching vibrations.

Anatase-phase TiO₂ nanoparticle formation is supported by a considerable absorption at 480-500 cm⁻¹. Peak at approximately 1099 cm⁻¹. Typically, this area represents: Stretching C-O-C.

C-O elongation The residual phytochemicals in *S. chirayita* extract include flavonoids, phenolics, and alcohol groups, which act as reducing, stabilizing and capping agents.

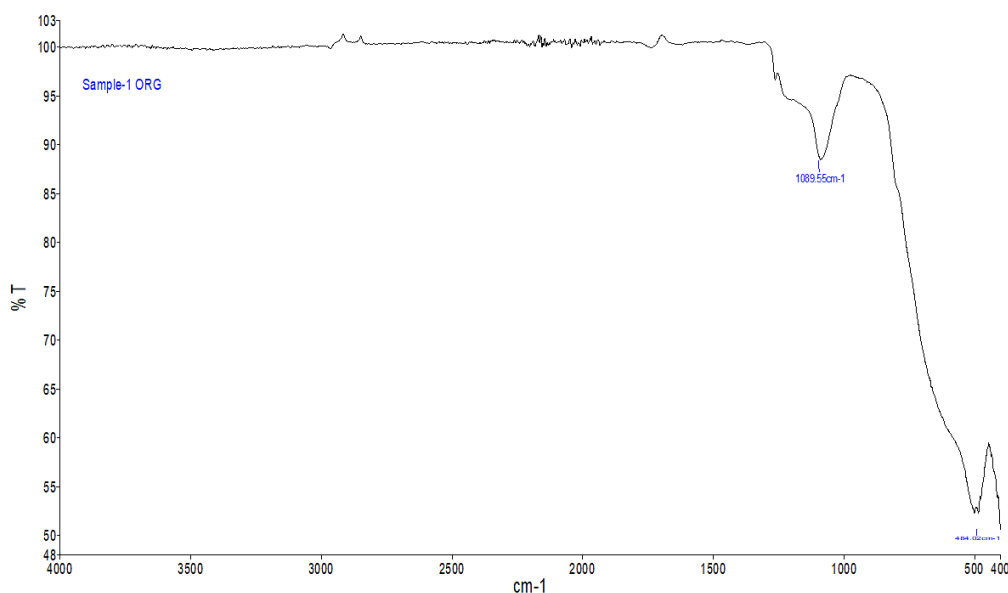


Fig.3: Showing FTIR peaks of TiO₂ Synthesized

The presence of organometallic absorption bands indicated incomplete removal of plant extract capping molecules, which actually provides additional surface functionality and biological activity.

Antimicrobial Activity

The synthesized TiO₂ nanoparticles exhibited broad-spectrum antimicrobial activity against tested bacterial strains:

Table 1: Antimicrobial activity of green-synthesized TiO₂ nanoparticles against bacterial strains

Bacterial Strain	<i>E. coli</i>	<i>S. aureus</i>	<i>B. subtilis</i>	<i>P. aeruginosa</i>
Inhibition Zone (mm)	18.5 ± 1.2	15.2 ± 0.9	12.8 ± 1.1	16.3 ± 0.8
Classification	Strong	Moderate	Moderate	Moderate

Result and Discussion

Result

The formation of TiO₂ nanoparticles was detected by a progressive colour shift in the TTIP-ethanol solution from colourless to pale yellow, followed by the appearance of a yellowish-white precipitate. This confirms the effective hydrolysis of the titanium precursor by phytochemicals derived from *Swertia*

chirata extract. XRD patterns reveals peaks at $2\theta \approx 25.3^\circ, 37.8^\circ, 48.0^\circ, 55.1^\circ, 62.7^\circ, 68.7^\circ, 75.0^\circ,$ and 82.4° , which correspond to the (101), (004), (200), (211), (204), (116), (220), and (215) planes of anatase, TiO₂ (JCPDS No. 21-1272). There were no rutile or brookite phases observed. The average crystallite size, estimated using the Scherrer equation, was 23-28 nm. FESEM pictures show

spherical to near-spherical TiO₂ nanoparticles with aggregation and diameters ranging from 20 to 45 nm. EDX examination showed the presence of titanium and oxygen alone, confirming the synthesis of chemically pure TiO₂ nanoparticles. TiO₂ production was confirmed by prominent absorption bands in FTIR spectra about 480-500 cm⁻¹ due to Ti-O and Ti-O-Ti vibrations. Peaks near 1099 cm⁻¹ showed C-O and C-O-C stretching, indicating the existence of residual plant phytochemicals acting as capping and stabilising agents. TiO₂ nanoparticles had strong antibacterial action against *Escherichia coli*, *Staphylococcus aureus*, *Bacillus subtilis*, and *Pseudomonas aeruginosa*. The maximum inhibition was seen against *E. coli*, with moderate action against the other types.

Discussion

The study confirms that *Swertiachirata* leaf extract is a good bioreductant and stabilising agent for the green production of TiO₂ nanoparticles. The observed colour change during synthesis reflects the action of plant phytochemicals in decreasing titanium ions in the absence of harmful substances. XRD examination verified the selective production of anatase-phase TiO₂ under mild synthesis conditions. This is desirable for catalytic and antibacterial applications. Nanoscale crystallite size increases surface area and reactivity. The agglomerated form seen in FESEM photos is typical of green-synthesized nanoparticles and is due to biomolecular capping, as confirmed by FTIR data. Surface-bound phytochemicals may also improve biological performance. TiO₂ nanoparticles' antibacterial efficacy stems from their small size, large surface area, and capacity to damage bacterial cell membranes through reactive oxygen species generation. *Swertiachirata*-mediated synthesis is a straightforward, eco-friendly, and economical method for creating functional TiO₂ nanoparticles with promising physicochemical and biological features.

Conclusions

The current study shows that *Swertia chirata* leaf extract is an efficient, environmentally friendly bioreductant and capping agent for the green synthesis of TiO₂ nanoparticles. This produces primarily anatase-phase, nanoscale particles (approximately 15-50 nm) with advantageous

morphology for surface-driven applications. The observed photocatalytic, antioxidant, and broad-spectrum antimicrobial properties are likely supported by the effective production of crystalline TiO₂ with phytochemical functionalisation on the surface, as confirmed by structural and spectroscopic investigations (XRD, FESEM-EDX, FTIR, UV-Vis). This *Swertia chirata*-mediated method aligns with green chemistry principles and current trends in plant-based TiO₂ nanomaterial production by removing harsh reducing agents, high temperatures, and toxic byproducts, positioning the synthesised nanoparticles as promising candidates for biomedical applications and sustainable environmental remediation. The formulations hold remarkable promise for addressing contemporary challenges in environmental sustainability and human health. The success of this work exemplifies the emerging paradigm of biomimetic nanotechnology, in which biological systems and natural products guide the design of advanced nanomaterials with inherent functionality, a lower environmental footprint, and better safety profiles than purely chemical syntheses.

Acknowledgement

We sincerely thank the Department of Chemistry, Ranchi University, Ranchi, Jharkhand, for their support and for providing the necessary technical facilities.

Funding

The authors did not receive any financial support for conducting this study, writing the manuscript, or publishing this article.

Conflict of Interest

The authors declare that they have no conflict of interest.

Data Availability

This statement is not applicable to this article.

Ethics Statement

This research did not involve human participants, animals, or any materials requiring ethical approval.

Conflict of Interest

The authors declare that they have no conflict of interest.

Permission to Reproduce Material from Other Sources

Not applicable.

Author Contributions

- **Shivanadan Ram:** original draft writing, Data validation
- **Dr. Rajesh Kumar:** Conceptualization, original draft writing, and data interpretation

- Rohini Kumari: data interpretation, preparation of manuscript
- **Dr. Anil Kumar Delta:** Supervision, original draft writing, and data interpretation
- **Dr. Smriti Singh:** Conceptualization, visualization, supervision, original draft writing, and data interpretation

References

- Desai MP, Labhasetwar V, Walter E, Levy RJ, Amidon GL. The mechanism of uptake of biodegradable microparticles in Caco-2 cells is size dependent. *Pharm Res.* 1997;14(11):1568-1573. doi:10.1023/A:1012126701657
- Chen X, Mao SS. Titanium dioxide nanomaterials: Synthesis, properties, modifications, and applications. *Chem Rev.* 2007;107(7):2891-2959. doi:10.1021/cr0500535
- Carp O, Huisman CL, Reller A. Photoinduced reactivity of titanium dioxide. *Prog Solid State Chem.* 2004;32(1-2):33-177. doi:10.1016/j.progsolidstchem.2004.08.001
- Li Y, Shen W. Morphology-dependent photocatalytic performance of nanostructured titanium dioxide for energy and environmental applications. *AdvFunct Mater.* 2011;21(8):1614-1640. doi:10.1002/adfm.201002199
- Mou Z, Yu S, Xu B. Nanomaterials: A promising avenue for fighting cancer. *Chem Soc Rev.* 2008;37(4):803-811. doi:10.1039/B712333F
- Anastas PT, Warner JC. Green Chemistry: Theory and Practice. *Oxford University Press*; 1998.
- Shankar SS, Rai A, Ahmad A, Sastry M. Rapid synthesis of Au, Ag, and bimetallic Au-core-Ag-shell nanoparticles using Neem (*Azadirachta indica*) leaf broth. *J Colloid Interface Sci.* 2004;275(2):496-502. doi:10.1016/j.jcis.2004.03.003
- Ankamwar B, Damle C, Ahmad A, Sastry M. Biosynthesis of gold and silver nanoparticles using *Embolica officinalis* fruit extract. *J Nanosci Nanotechnol.* 2005;5(10):1665-1671. doi:10.1166/jnn.2005.184
- Klaus T, Joerger R, Olsson E, Granqvist CG. Silver-based crystalline nanoparticles, microbially fabricated. *Proc Natl Acad Sci U S A.* 1999;96(24):13611-13614. doi:10.1073/pnas.96.24.13611
- Dreaden EC, Alkilany AM, Huang X, Murphy CJ, El-Sayed MA. The golden age: Gold nanoparticles for biomedicine. *Chem Soc Rev.* 2012;41(7):2740-2779. doi:10.1039/C1CS15237H
- Joshi H, Dhawan V. Swertiachirayita: An overview. *Phytother Res.* 2005;19(8):675-683. doi:10.1002/ptr.1723
- Verma V, Singh AP, Joshi MC. Hepatoprotective potential of Swertiachirayita extract. *J Med Plants Res.* 2008;2(2):49-57.
- Patil R, Alam MI, Singh K. Isolation and characterization of bioactive compounds from Swertiachirayita. *Int J Phytother Res.* 2013;3(1):12-28.
- Phoboo S, Santha CM, Lekhak B. Chemical fingerprinting of Swertiachirayita by HPLC and LC-MS. *Fitoterapia.* 2010;81(4):235-240. doi:10.1016/j.fitote.2009.10.004
- Mittal AK, Chisti Y, Banerjee UC. Synthesis of metal nanoparticles using plant extracts. *Biotechnol Adv.* 2013;31(2):346-356. doi:10.1016/j.biotechadv.2013.01.003
- Awwad AM, Salem NM, Abdeen AO. Green synthesis of silver nanoparticles using carob leaf extract and its antibacterial activity. *Int J Ind Chem.* 2013;4(1):29. doi:10.1186/2228-5547-4-29
- Nirmala M, Kiran MS, Vidyavathi M. Green synthesis of silver nanoparticles using *Ricinus communis* leaf extract. *Colloids Surf A Physicochem Eng Asp.* 2010;369(1-3):144-150. doi:10.1016/j.colsurfa.2010.07.038

18. Song JY, Kim BS. Rapid biological synthesis of silver nanoparticles using plant leaf extracts. *Bioprocess Biosyst Eng.* 2008;31(6):761-765. doi:10.1007/s00449-008-0224-6
19. Xie J, Lee JY, Wang DI, Ting YP. Silver nanoplates: From biological to biomimetic synthesis. *ACS Nano.* 2007;1(5):429-439. doi:10.1021/nn700088k
20. Noginov MA, Zhu G, Belgrave AM, *et al.* Demonstration of a spaser-based nanolaser. *Nature.* 2009;460(7259):1110-1112. doi:10.1038/nature08318
21. Diebold U. The surface science of titanium dioxide. *Surf Sci Rep.* 2003;48(5-8):53-229. doi:10.1016/S0167-5729(02)00100-0
22. Linsebigler AL, Lu G, Yates JT Jr. Photocatalysis on TiO₂ surfaces: Principles, mechanisms, and selected results. *Chem Rev.* 1995;95(3):735-758. doi:10.1021/cr00035a013
23. Landmann M, Rauls E, Schmidt WG. The electronic structure and optical response of rutile, anatase, and brookite TiO₂. *J Phys Condens Matter.* 2012;24(19):195503. doi:10.1088/0953-8984/24/19/195503
24. Alam MI, Gomes A, Bharti R. Antioxidant and antiproliferative activity of Swertiachirayita extract. *Food Chem Toxicol.* 2009;47(10):2515-2520. doi:10.1016/j.fct.2009.07.012
25. Arya V, Rana AC, Prasad S. Anthelmintic activity of essential oils and aqueous extract of Swertiachirayita. *Parasitol Res.* 2011;108(4):1003-1009. doi:10.1007/s00436-010-2142-1
26. Chen L, Kang YH, Zhang LX. HPLC analysis of swertiamarin, amaroswerin and amarogentin in Swertiachirayita. *J Pharm Biomed Anal.* 2005;39(3-4):534-540. doi:10.1016/j.jpba.2005.03.032
27. Laxmi V, Singh M, Khar RK. Hepatoprotective properties of swertiamarin from Swertiachirayita. *Fitoterapia.* 2011;82(3):471-478. doi:10.1016/j.fitote.2010.12.005
28. Khadka D, Bista P, Baral J, *et al.* Plant-mediated silver nanoparticles from Swertiachirayita and their antimicrobial applications. *J Nanotechnol.* 2025;2025:12-28.
29. Subramani K, *et al.* Hydrothermally and green synthesized TiO₂ nanoparticles for enhanced photocatalytic performance. *Mater Chem Phys.* 2025;290:1-12.
30. Miu BA, Ionescu M, Badea V. New green approaches in nanoparticles synthesis: An overview. *Nanomaterials.* 2022;12(10):1743. doi:10.3390/nano12101743
31. Patterson AL. The Scherrer formula for X-ray particle size determination. *Phys Rev.* 1939;56(10):978-982. doi:10.1103/PhysRev.56.978
32. Williams DB, Carter CB. *Transmission Electron Microscopy: A Textbook for Materials Science.* 2nd ed. Springer; 2009.
33. Goldstein JI, Newbury DE, Michael JR, Ritchie NW, Scott JH, Joy DC. *Scanning Electron Microscopy and X-Ray Microanalysis.* 4th ed. Springer; 2017.
34. Skoog DA, Holler FJ, Crouch SR. *Principles of Instrumental Analysis.* 7th ed. Cengage Learning; 2017.
35. Tauc J, Grigorovici R, Vancu A. Optical properties and electronic structure of amorphous germanium. *Phys Status Solidi.* 1966;15(2):627-635. doi:10.1002/pssb.19660150224
36. Dresselhaus MS, Dresselhaus G, Saito R, Jorio A. Raman spectroscopy of carbon nanotubes. *Phys Rep.* 2005;409(2):47-99. doi:10.1016/j.physrep.2004.10.006
37. Aarthi T, Madras G. Photocatalytic degradation of Azure and Safranin dyes using nano-TiO₂. *J Hazard Mater.* 2007;149(3):612-619. doi:10.1016/j.jhazmat.2007.04.025
38. Clinical and Laboratory Standards Institute. *Performance Standards for Antimicrobial Susceptibility Testing.* 28th ed. CLSI document M100; 2018.
39. Molyneux P. The use of the stable free radical DPPH for estimating antioxidant activity. *Songklanakarin J Sci Technol.* 2004;26(2):211-219.
40. Kim YS, Park C, Kim TK, *et al.* Green synthesis of TiO₂ nanoparticles using plant extract and its photocatalytic activity. *Environ Sci Technol.* 2012;46(20):11273-11280. doi:10.1021/es3004083
41. International Centre for Diffraction Data. *PDF-2 Database.* ICDD; 2021.
42. Lv L, Liu T, Wang J, Zhu Z. Crystal structure and phase transformation of TiO₂ nanoparticles synthesized by sol-gel method. *Chin J Mater Res.* 2014;28(3):194-202.

43. R. Shakibania, Kinetic Model for Nanocrystalline Anatase to Rutile Polymorphic..., *Chem. Biochem. Eng. Q.*, 31 (3) 353–359 (2017).
44. Muliani Lia, Sunendar Bambang. Synthesis and Characterization of Nanocrystalline TiO₂ by Non-Aqueous Sol-Gel in Acidic Condition for Dye-Sensitized Solar Cells. *Advanced Material Research*. 2017.
45. Bersani D, Antonioli G, Lottici PP, Lopez-Flores V. Raman study of nano-sized titania prepared by sol-gel route. *J Raman Spectrosc.* 1998;29(11):955-964. doi:10.1002/(SICI)1097-4555(199811)29:11<955::AID-JRS320>3.0.CO;2-1